The use of *FT*i.r.–a.t.r. spectroscopy to characterize penetrant diffusion in polymers

G. T. Fieldson and T. A. Barbari*
Department of Chemical Engineering, The Johns Hopkins University, Baltimore, MD 21218, USA
(Received 10 July 1992; revised 11 August 1992)

The diffusion of small molecules in polymers was measured using Fourier transform infra-red–attenuated total reflection (*FT*i.r.–a.t.r) spectroscopy, a new approach which allows one to study liquid diffusion in thin polymer films *in situ*. The system used to test this technique was the diffusion of liquid water in polyacrylonitrile (PAN). The diffusion coefficients that were measured were in good agreement with those reported in the literature for high-activity water vapour in PAN. The test also demonstrated both the reproducibility and accuracy of *FT*i.r.–a.t.r. experiments for measuring the diffusion coefficient. The diffusion coefficient and the amount of water sorbed at equilibrium appear to be dependent on the temperature at which the films were treated. The method described here shows great potential for elucidating penetrant–penetrant and penetrant–polymer interactions during the diffusion process owing to the spectroscopic nature of the technique.

(Keywords: *FT*i.r.–a.t.r. spectroscopy; diffusion; polyacrylonitrile; water)

BACKGROUND

Diffusion in polymers

For one-dimensional molecular diffusion in a polymer film with a constant diffusion coefficient, the continuity equation for the diffusing species reduces to:

$$\frac{\partial C}{\partial t} = D\frac{\partial^2 C}{\partial z^2} \tag{1}$$

where C is the concentration of penetrant and D is the diffusion coefficient. Equation (1) can be solved readily, given the appropriate boundary conditions that apply to a particular experiment.

One of the most common experimental techniques for studying the diffusion of small molecules in polymers is the method of sorption kinetics. In this technique, a polymer film of thickness $2L$ is placed in an infinite bath of penetrant. The concentrations at the two surfaces of the film ($z = L$ and $z = -L$) are instantaneously established at a concentration, C_s. If the initial concentration of penetrant is zero, then the concentration, C, at any position in the film, z, and at any time, t, is given by[1]:

$$\frac{C}{C_s} = 1 - \frac{4}{\pi}\sum_{n=0}^{\infty}\frac{(-1)^n}{2n+1}\exp\left[\frac{-D(2n+1)^2\pi^2 t}{4L^2}\right] \times \cos\left[\frac{(2n+1)\pi z}{2L}\right] \tag{2}$$

In sorption kinetics experiments, the mass of sorbed penetrant is measured as a function of time. The sorbed mass is obtained by integrating equation (2) over the thickness of the film. The result of this integration is:

$$\frac{M_t}{M_\infty} = 1 - \sum_{n=0}^{\infty}\frac{8}{(2n+1)^2\pi^2}\exp\left[\frac{-D(2n+1)^2\pi^2 t}{4L^2}\right] \tag{3}$$

where M_t is the mass sorbed at time t, and M_∞ is the mass sorbed at equilibrium. At short times, equation (3) can be written, for a thickness of $2L$, as:

$$\frac{M_t}{M_\infty} = \frac{2}{L}\left(\frac{D}{\pi}\right)^{1/2} t^{1/2} \tag{4}$$

A typical plot of M_t/M_∞ as a function of $t^{1/2}$ is shown in *Figure 1*. The linear portion of the curve is used to determine the diffusion coefficient using equation (4). At $M_t/M_\infty \leqslant 0.5$, the error in using equation (4) instead of equation (3) is on the order of 0.1%[2].

Depending on the film thickness and the diffusion coefficient, there may be limited data at $M_t/M_\infty \leqslant 0.5$. In these situations, the long-time solution:

$$\frac{M_t}{M_\infty} = 1 - \frac{8}{\pi^2}\exp\left(\frac{-D\pi^2 t}{4L^2}\right) \tag{5}$$

can be used, usually in the form:

$$\ln\left(1 - \frac{M_t}{M_\infty}\right) = \ln\left(\frac{8}{\pi^2}\right) - \frac{D\pi^2 t}{4L^2} \tag{6}$$

A mass uptake plot, in the form of equation (6), is shown in *Figure 2*. At $M_t/M_\infty \geqslant 0.5$, the error in using equation (6) instead of equation (3) is also on the order of 0.1%[2].

Fickian diffusion with a concentration-dependent diffusion coefficient can also result in curves similar to those shown in *Figures 1* and *2*. The resulting value of

---

* To whom correspondence should be addressed

0032-3861/93/061146–08

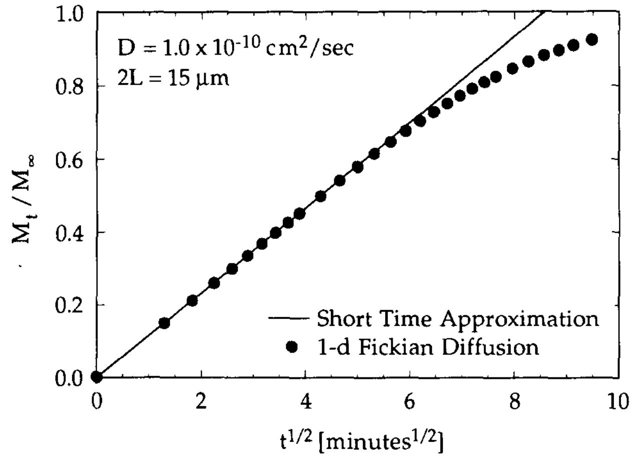

Figure 1 M_t/M_∞ *versus* $t^{1/2}$ for one-dimensional Fickian diffusion

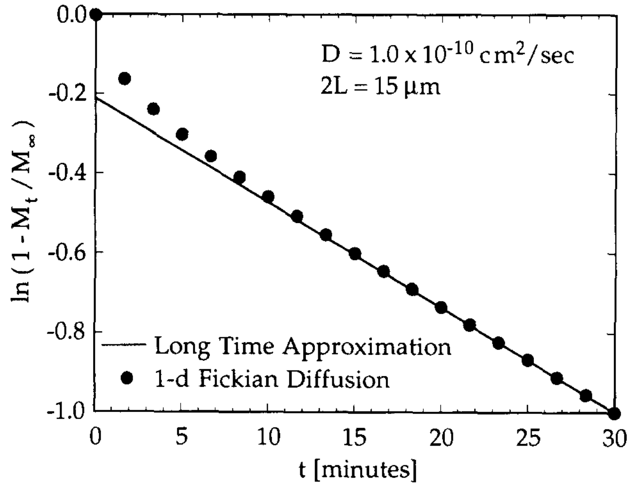

Figure 2 $\ln(1 - M_t/M_\infty)$ *versus* t for one-dimensional Fickian diffusion

D determined through equation (4) (*Figure 1*) or equation (6) (*Figure 2*) is an average value over the applicable concentration range.

Sorption kinetics experiments are commonly used to determine diffusion coefficients for penetrants in polymers. For non-condensable gases such as methane, nitrogen and carbon dioxide, pressure decay techniques are often used to monitor sorption kinetics[3–5]. For more condensable gases or vapours, gravimetric techniques that directly follow mass changes with time are used[6–8]. Polymer samples are mounted on a quartz spring microbalance and the change in mass is recorded as a function of time. The recorded weight is corrected for buoyancy to obtain the mass of the sample. This technique can be extremely accurate provided a sensitive microbalance is used.

Quartz spring microbalances are difficult to apply to liquid sorption kinetics. Since the density of the liquid medium is close to the density of the polymer, correction for buoyancy results in considerably less accurate values of sorbed mass. Instead, so-called 'pat-and-weigh' techniques are used for liquid sorption. This involves immersing the polymer in the liquid penetrant and periodically removing the sample, blotting the surfaces to remove excess liquid, and then weighing the sample on a conventional laboratory balance. If the sample is too thin or the diffusion coefficient is too high, a significant amount of penetrant may desorb during the time it is not immersed. This can be remedied by using thicker samples, but this can significantly increase the time required for a single experiment. The repeated handling of the sample can result in an erroneous rate of mass uptake.

The experimental method described here is designed primarily to measure liquid sorption kinetics *in situ*, but the technique is also suitable for gases or vapours. The approach utilizes quantitative Fourier transform infra-red–attenuated total reflection (*FT*i.r.–a.t.r.) spectroscopy to determine the amount of penetrant that has sorbed as a function of time. In addition to the sorption kinetics, a spectroscopic technique also provides information regarding the molecular state of the penetrant at various times in the diffusional process. The method can be applied to systems of thin polymer films with penetrants that are spectroscopically active, including multi-component systems, provided each penetrant absorbs in a unique region of the infra-red spectrum.

FT*i.r.–a.t.r. spectroscopy applied to diffusion in polymers*

The root of applied spectroscopy is the basic relationship between the absorption of electromagnetic waves and the quantity of the absorbing material. In *FT*i.r. transmission spectroscopy at low absorbances, this relationship is expressed by the Beer–Lambert law given by:

$$dI = \alpha I \, dz = -\varepsilon C I \, dz \qquad (7)$$

where I is the light intensity at position z, α is the absorption coefficient, ε is the molar extinction coefficient and C is the concentration of absorbing group.

Integrating equation (7) gives:

$$A = -\ln\left\{\frac{I}{I_0}\right\} = \int_{-L}^{L} \varepsilon C \, dz \qquad (8)$$

where A is the measured absorption, I_0 is the intensity of the incident light, I is the intensity of the transmitted light and $2L$ is the thickness over which the absorbing group is present.

The absorbance given in equation (8) is analogous to the mass uptake in equation (3) since it involves an integration of the concentration profile over the film thickness. Using transmission spectroscopy to measure sorption kinetics with equation (8) suffers from many of the same limitations that are inherent in the 'pat-and-weigh' technique. The polymer must be removed from the penetrant bath and blotted prior to spectroscopic analysis. Although it may provide molecular information about the state of the penetrant, transmission *FT*i.r. cannot be used to measure small-molecule sorption kinetics *in situ*.

However, by the nature of the experimental arrangement, *FT*i.r.–a.t.r. spectroscopy can be used to obtain sorption kinetics while in direct contact with the penetrant. A.t.r. spectroscopy differs from normal transmission spectroscopy in the nature of the incident light path. When total reflection of a light beam occurs at the boundary between a propagating medium (an a.t.r. crystal) and a rarer medium (a polymer film), penetration of the electromagnetic field into the rarer medium occurs. This electromagnetic field forms an evanescent wave, which is the result of the superposition of the incident and reflected waves at the surface, and the requirement that the electric field be continuous through the

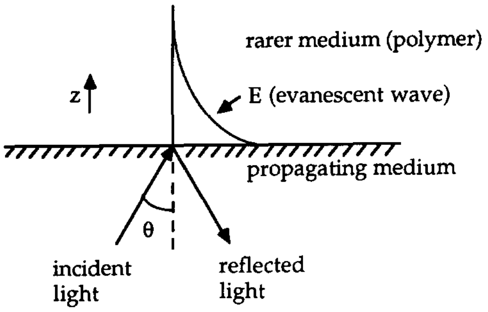

Figure 3 Evanescent wave at a totally reflecting interface

interface[9,10]. The electric field strength, E, of the evanescent wave decays exponentially, as shown in *Figure 3*, with distance from the surface, z.

The decay of the evanescent field is given by[9,10]:

$$E = E_0 \exp(-\gamma z) \qquad (9)$$

where E_0 is the electric field strength at the interface and γ is defined as the reciprocal of the penetration depth, the distance to which the evanescent wave decays to $1/e$ of its value at the interface. In terms of refractive indices, wavelength (λ), and the angle of incidence (θ), γ is given by:

$$\gamma = \frac{2n_2\pi\sqrt{\sin^2\theta - \left(\frac{n_1}{n_2}\right)^2}}{\lambda} \qquad (10)$$

where n_1 is the refractive index of the rarer medium and n_2 is the refractive index of the propagating medium.

When the rarer medium absorbs specific frequencies of light in the evanescent wave, the reflection is frustrated and the reflected wave has a reduced intensity at these wavelengths, resulting in an absorption spectrum. In order to combine the evanescent field strength equation with the Beer–Lambert law, it is necessary to assume that only weak absorption occurs. With this assumption:

$$\frac{I}{I_0} = e^{-A} \approx (1 - A) \qquad (11)$$

or

$$\mathrm{d}I = -I_0\,\mathrm{d}A \qquad (12)$$

We can substitute equation (12) into the differential form of the Beer–Lambert law (equation (6)) and integrate to obtain:

$$A = \int_0^L \frac{\varepsilon C I}{I_0}\,\mathrm{d}z \qquad (13)$$

In the a.t.r. configuration, penetrant only enters the film from one side, hence the integration from 0 to L. Since $I = E^2$, we can substitute the field strength of the evanescent wave (equation (9)) and rewrite the expression for multiple reflections, N, as:

$$A = \int_0^L N\varepsilon^* C E_0^2 \exp(-2\gamma z)\,\mathrm{d}z \qquad (14)$$

where $\varepsilon^* = \varepsilon / I_0$.

Substituting equation (2), the Fickian concentration profile, into equation (14) and integrating gives:

$$\frac{A_t}{A_\infty} = 1 - \frac{8\gamma}{\pi[1 - \exp(-2\gamma L)]} \times \sum_{n=0}^{\infty}\left[\frac{\exp(g)[f\exp(-2\gamma L) + (-1)^n(2\gamma)]}{(2n+1)(4\gamma^2 + f^2)}\right] \qquad (15)$$

where

$$g = \frac{-D(2n+1)^2\pi^2 t}{4L^2}$$

and

$$f = \frac{(2n+1)\pi}{2L}$$

Equation (15) is analogous to the mass uptake equation used in gravimetric sorption experiments (equation (3)), the important difference being that the Fickian concentration profile is convoluted with the *FT*i.r.–a.t.r. absorption equation before it is integrated. In equation (15), A_∞ represents the absorbance at equilibrium and it is analogous to M_∞.

Equation (15) represents an exact solution for *FT*i.r.–a.t.r. absorption of a penetrant in a thin film. It is possible, for a particular set of experimental conditions, to simplify this expression. For the experimental system described in this paper, several assumptions and resulting simplifications of equation (15) were made.

Simplification of the FT*i.r.–a.t.r. model*

Equation (15) can be simplified by eliminating all terms in the series beyond the first:

$$\frac{A_t}{A_\infty} = 1 - \frac{8\gamma}{\pi[1 - \exp(-2\gamma L)]} \times \left[\frac{\exp\left(\frac{-D\pi^2 t}{4L^2}\right)\left(\frac{\pi}{2L}\exp(-2\gamma L) + (2\gamma)\right)}{\left(4\gamma^2 + \frac{\pi^2}{4L^2}\right)}\right] \qquad (16)$$

For values of L, D and γ which are typical for the experimental system used here, absorbances from equation (16) are compared to those from equation (15) and shown in *Figure 4*. It is obvious that the first-order term dominates the absorbance expression at values of $A_t/A_\infty \geqslant 0.5$. This result is identical to the observation that the mass uptake described by equation (3) can be approximated by equation (5) for values of $M_t/M_\infty \geqslant 0.5$.

In the model development, γ is assumed to be constant. This is not entirely correct, given the dependence of γ on n_1, the polymer refractive index, which can vary as the concentration of penetrant increases. However, the significance of γ in the model is dependent on the experimental conditions. In particular, when

$$4\gamma^2 \gg \frac{\pi^2}{4L^2} \qquad (17)$$

and

$$1 \gg \exp(-2\gamma L) \qquad (18)$$

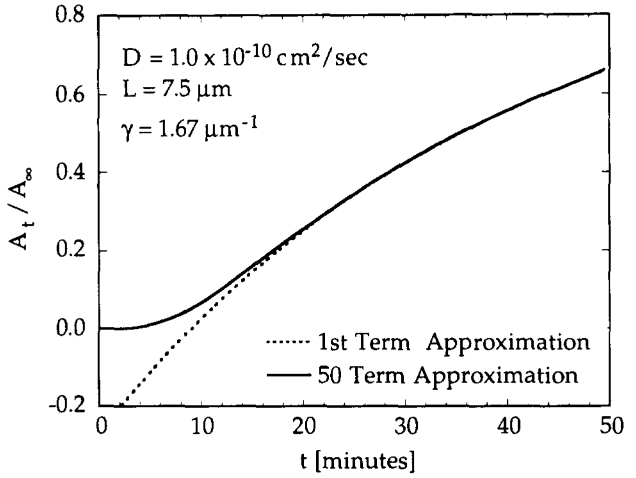

Figure 4 Comparison of full a.t.r. expression (equation (15)) and first term approximation (equation (16))

γ can be eliminated from equation (16). This requirement is readily met for most experimental systems.

Under these conditions, equation (16) can be reduced to the expression:

$$\ln\left(1-\frac{A_t}{A_\infty}\right)=\ln\left(\frac{4}{\pi}\right)-\frac{D\pi^2}{4L^2}t \qquad (19)$$

With equation (19), the logarithm of the absorbance data is plotted as a function of time, and the slope of a linear least squares regression yields a value for the diffusion coefficient, D. This is wholly analogous to the use of equation (6) to determine the diffusion coefficient in gravimetric sorption experiments at long times.

The value of A_∞ can be measured independently or it can be calculated by regression as a second adjustable parameter in addition to the diffusion coefficient. While it is desirable to measure A_∞ independently and treat equation (19) as a one-parameter model, experimental conditions may make accurate determinations of the equilibrium infra-red absorption unreliable or impossible, as will be discussed in detail below.

Experimental test system

The experimental system chosen to test this *FT*i.r.–a.t.r. spectroscopic technique was the diffusion of water in polyacrylonitrile (PAN). This system was chosen for several reasons. The most important reason was the availability of diffusion coefficients reported in the literature for high-activity water vapour in PAN at similar temperatures[11–13]. Additionally, PAN has a relatively sparse infra-red absorption spectrum. This minimizes the possibility of spectral interference between the substrate and the penetrant. The magnitudes of the diffusion coefficient and the solubility of water in PAN are also favourable for these types of measurements. Water has a total solubility of 3–5% in PAN by weight, and a diffusion coefficient which suggests that sorption of water in films 5–10 μm thick is completed within a few hours, a period conducive to laboratory measurement.

PROCEDURES

Polymer film preparation procedures

The polymer films are prepared on a Headway Research EC-110 spin coater. The spin coater has the ability to regulate its rotational velocity from 50 to 5000 rev min^{-1}. The spin coater cabinet is equipped with a cover which is used to maintain a dry nitrogen atmosphere over the sample. This nitrogen is obtained from the vent gases of the liquid nitrogen supply used to cool the infra-red detector of the *FT*i.r. spectrometer.

A film is cast by spin coating a polymer solution at room temperature. Approximately 1 ml of the solution is placed on an a.t.r. crystal in the spin coater, and the sample is rotated for 15–30 min. The rotational velocity of the spin coater is chosen such that a uniform, reproducible polymer film of desired thickness is obtained. After spin coating, the crystal and film are transferred to a vacuum oven.

The film, along with the a.t.r. cell and steel connecting tubes, is placed in a vacuum oven to remove residual solvent or condensed water, and to condition or anneal the polymer film. The films are kept in the oven for at least 24 h at various temperatures. At the end of this time, the film and crystal are transferred to a desiccator and allowed to cool to room temperature. The a.t.r. cell and tubing are removed and placed on the spectrometer bench, where they are also allowed to cool to room temperature.

FT*i.r.–a.t.r. spectroscopy procedures*

Measurements of the infra-red spectra are obtained using a Mattson Galaxy® 6020 *FT*i.r. spectrometer. The spectrometer is capable of scanning with a resolution of up to 0.25 cm^{-1}, and is equipped with a wide-band mercury–cadmium–tellurium (MCT) detector. The spectrometer is controlled from an IBM compatible PC (Dell system 310) running Mattson's FIRST® software. The a.t.r. crystals used in the experiments are polished silicon parallelepipeds, obtained from Harrick Scientific, Inc. The sampling surfaces of the crystals are 50 mm × 10 mm and they have a thickness of 3 mm. The normal vectors of the optical entry and exit faces are inclined 30° from the sampling surfaces. The refractive index of silicon is 3.4.

Once the film-coated crystal has cooled to room temperature, it is mounted in a flow-through a.t.r. cell obtained from Harrick Scientific, Inc., as shown in *Figure 5*. After the cell is closed, excess polymer film on the entry and exit faces of the crystal is removed. In the a.t.r. cell, the solvent flows through one side of the cell and across the polymer film, while temperature-controlled water can be passed across the other side of the cell to regulate the temperature of the crystal. The back of the crystal is masked with aluminium foil to

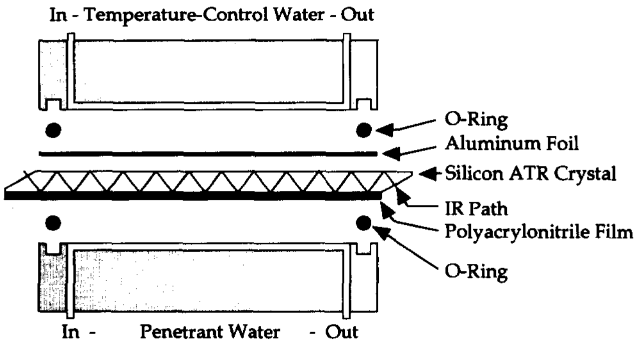

Figure 5 Exploded view of a.t.r. cell

prevent infra-red absorption by the temperature-controlled water. The exposed area of the polymer sample within the liquid cell is 6 mm × 42 mm.

The cell is placed in the variable-angle a.t.r. holder as shown in *Figure 6*, also obtained from Harrick Scientific, Inc., and the second mirror of the holder is rotated slightly, as necessary, to align the sample. The entire base assembly is then mounted in the spectrometer sample compartment, and the steel tubing for the sample feed and the temperature-controlled water is attached. Final alignment of the second mirror is performed by maximizing the voltage at the MCT detector, and the compartment is closed and purged with nitrogen gas. The effectiveness of the purge is monitored by examining the carbon dioxide absorption in the infra-red spectrum. The external fittings of the tubing attached to the cell are connected to the penetrant reservoir and the temperature-controlled circulating bath. The experimental configuration is shown in *Figure 7*.

Control of the spectrometer for collection of the spectra is performed with Mattson's FIRST®/Data Acquisition software. The spectrometer is operated in g.c./*FT*i.r. mode, allowing samples to be collected continuously. First, a background spectrum of the film is taken as a reference. The g.c./*FT*i.r. sampling process is then started, and the penetrant circulating pump is turned on.

Upon completion of the spectral sampling, the variable angle holder and cell are dismounted from the spectrometer. The crystal is removed from the liquid cell and examined visually for defects or delamination. The crystal is allowed to dry, and then the film is removed from the crystal, labelled and stored. The thickness of the films was measured mechanically, using a micrometer, after the diffusion experiment. Given the low sorption levels of water in PAN, it is assumed that the thickness of the film is not altered significantly during the experiment.

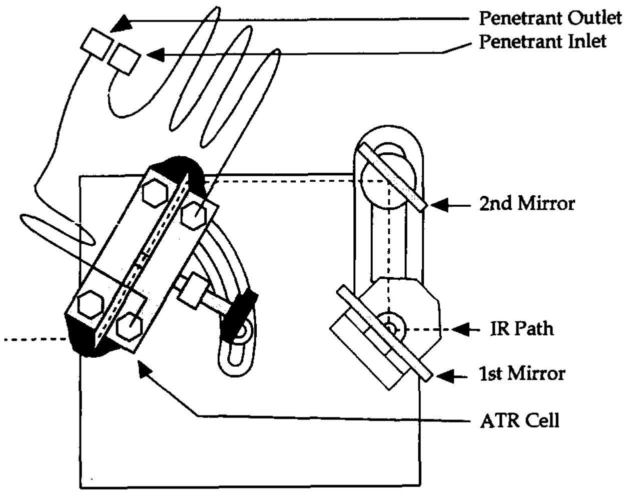

Figure 6 View of a.t.r. cell in variable-angle holder

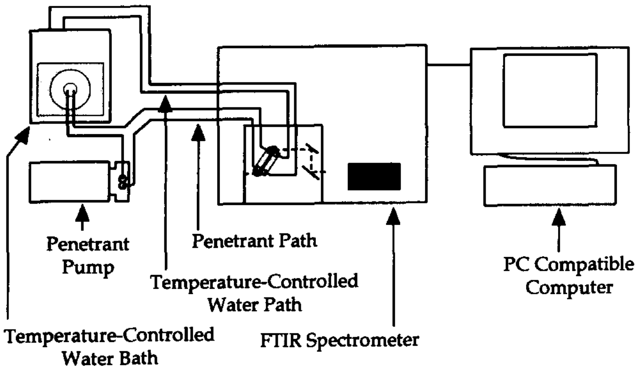

Figure 7 Experimental configuration for *FT*i.r.–a.t.r. spectroscopy

Evaluating FT*i.r.—a.t.r. data*

The first step of data analysis is the quantification of spectral information for use in the *FT*i.r.–a.t.r. model. The appropriate absorption peak is integrated and combined with the elapsed time of the experiment. The diffusion coefficient and A_∞ are obtained by regressing the experimental data, using equation (19). The parameter regression is done by determining the A_∞ which yields the minimum least-squared error for a linear least-squares regression of D. After the minima are located, the 99% confidence limits for the regression are calculated.

Experimental test materials and parameters

The PAN was obtained from Scientific Polymer Products, Inc. The polymer has a reported average molecular weight of 150 000. The refractive index of PAN is 1.5187, as reported by the supplier. The glass transition temperature was determined to be 85–90°C using differential scanning calorimetry at 20°C min^{-1}, which is in agreement with values reported in the literature[14]. The water used in the experiments was purified by reverse osmosis and ion exchange. The measured conductivity of the water was 7.0 μS cm^{-1}. Dimethylformamide (DMF) of technical grade, purchased from Aldrich, was used as a solvent in casting the PAN films.

The polymer solution used as stock for spin coating was approximately 8 wt% PAN. The spin coating of PAN on the silicon a.t.r. crystals was performed at a rotational velocity of 330 rev min^{-1} for 20 min. Each film was held under vacuum in the oven for a period of 24 h.

The parameters for the infra-red sampling are given in *Table 1*. The diffusion of water in the PAN films was measured by observing the OH stretching peak. The peak was integrated from 2775 to 3800 cm^{-1} to obtain an absorbance at each time.

RESULTS

Diffusion experiments for the water–PAN system at 23°C were conducted on PAN films which were vacuum treated for 24 h at temperatures of 57, 69, 80, 92 and 102°C. The thickness of the films was measured and determined to be 7.5 ± 2.5 μm. For the experimental conditions used here, $\gamma = 1.67\ \mu\text{m}^{-1}$ at 3500 cm^{-1}, and the criteria in

Table 1 *FT*i.r. spectrometer sampling parameters

Resolution	4 cm^{-1}
Starting frequency	1300 cm^{-1}
Ending frequency	4000 cm^{-1}
Scans per sample	55
Signal gain	20
Scan velocity	1.3 cm s^{-1}
Sampling time	27 s

equations (17) and (18) were met. A representative sample of the spectra recorded is shown in *Figure 8*.

The integrated absorbances for all of the experiments as a function of time are shown in *Figure 9*. The simplified *FT*i.r.–a.t.r. absorbance model (equation (19)) was regressed with the long time data to calculate values for each of the parameters in the model, D and A_∞. The value of A_∞ was obtained by regression instead of through a separate measurement, because visual inspection of some of the experimental films (those treated at lower temperatures) suggested that the polymer film had possibly become detached from the crystal after exposure to water for very long periods of time. Such detachment would make an equilibrium spectroscopic measurement unreliable. The likelihood confidence interval for each parameter was also calculated. The results of these calculations are given in *Table 2*. A comparison of the model and the experimental data is shown for two representative experiments in *Figure 10*.

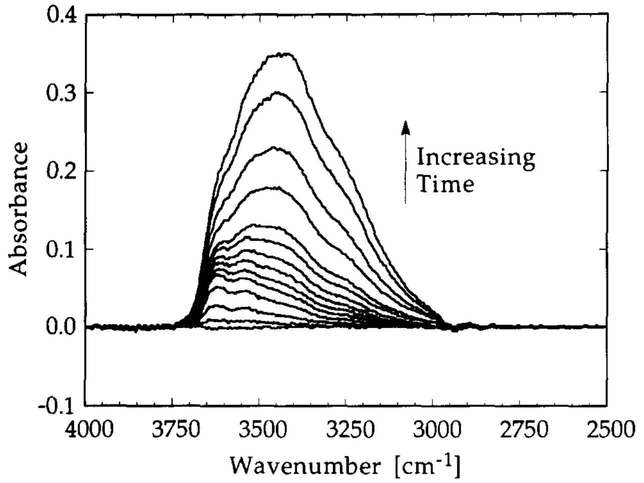

Figure 8 Sequence of time-evolved spectra from PAN sample treated at 102°C

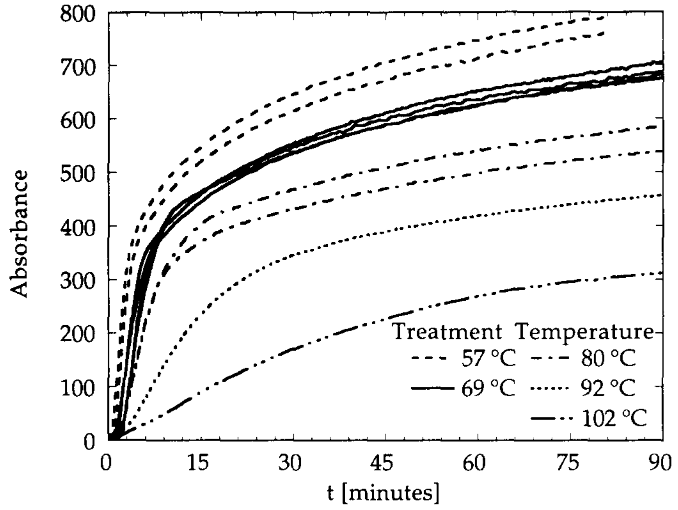

Figure 9 Integrated absorbance *versus* time for all test experiments of water–PAN at 23°C

The degree of solvent removal in the treatment process was estimated by comparison of the background spectra from each sample with a reference sample of DMF in carbon tetrachloride, and with a reference sample of a bare silicon crystal. The results are shown in *Figure 11*, where it is seen that a significant amount of solvent remained in most of the polymer films and that, not surprisingly, the degree of solvent removal was strongly related to the treatment temperature.

Figure 12, which shows the relationship between the average diffusion coefficient at long times and the treatment temperature, demonstrates that the long-time diffusion coefficient increases slightly at higher oven temperatures. Multiple data points at the same temperature have been spread apart in *Figure 12* for clarity; the exact values for each experiment are as given in *Table 2*. The absorbance at equilibrium, A_∞, which is directly proportional to the total amount of water sorbed in the polymer, appears to decrease in a linear fashion with the treatment temperature, as shown in *Figure 13*. Again, multiple samples at the same temperature have been spread apart for clarity. Repeated experiments at

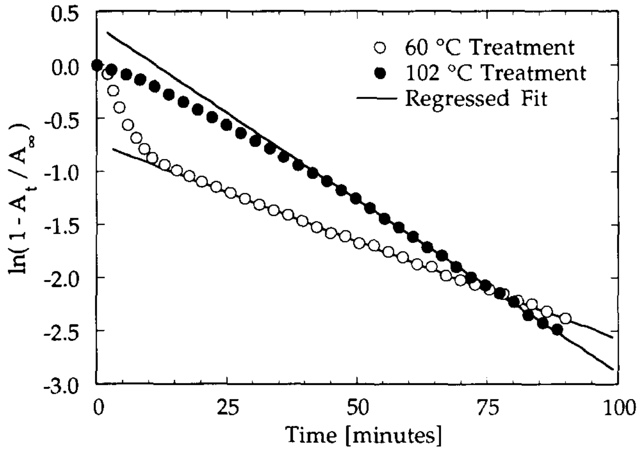

Figure 10 Comparison of model and representative data

Table 2 Results of regression of experimental data, with 99% confidence intervals

Treatment temperature, measured value (°C)	$D \times 10^{10}$ (cm^2 s^{-1})		A_∞	
	Regressed value	99% confidence interval	Regressed value	99% confidence interval
102	1.236	1.183–1.285	337.55	335.65–339.77
92	0.852	0.820–0.882	496.04	493.34–499.10
80	0.632	0.610–0.652	653.20	649.50–657.42
80	0.646	0.628–0.664	599.50	596.70–602.57
69	0.664	0.595–0.719	762.15	752.25–777.60
69	0.669	0.604–0.723	757.37	747.17–772.50
69	0.698	0.674–0.722	743.53	739.53–748.16
69	0.722	0.684–0.756	774.35	768.45–781.76
57	0.760	0.721–0.795	874.01	867.61–881.80
57	0.605	0.520–0.666	876.87	860.17–906.96

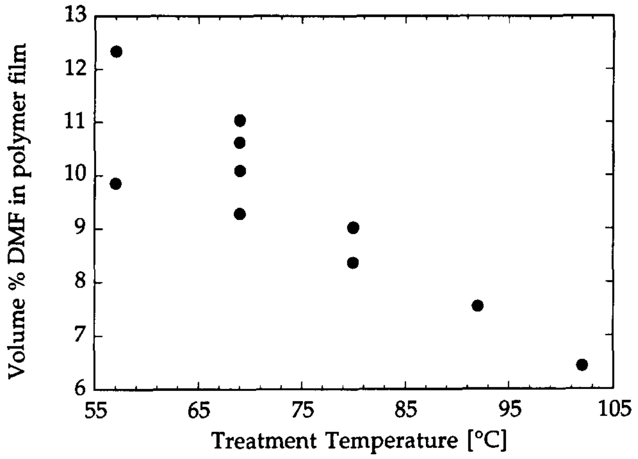

Figure 11 Volume per cent of residual DMF in PAN films *versus* treatment temperature

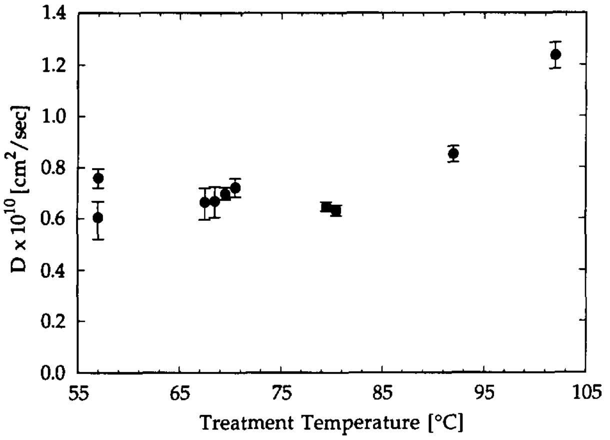

Figure 12 Average diffusion coefficient *versus* treatment temperature (data points at same temperature have been spread for clarity)

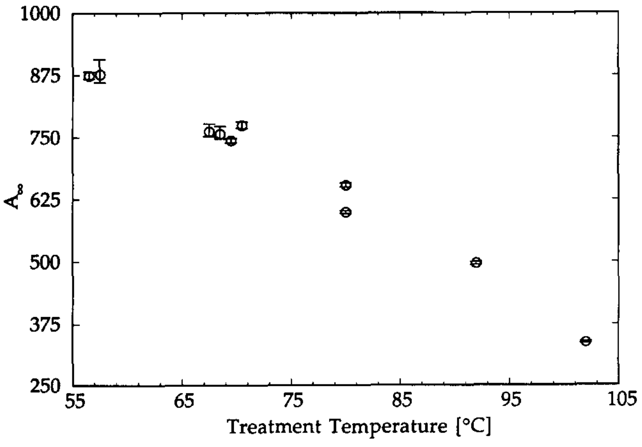

Figure 13 A_∞ *versus* treatment temperature (data points at same temperature have been spread for clarity)

57, 60 and 80°C yield only small deviations in the regressed values of D and A_∞, demonstrating that the *FT*i.r.–a.t.r. measurements are reproducible.

DISCUSSION

The results obtained in the test experiments agree favourably with values of the diffusion coefficient for water in PAN, from gravimetric techniques, reported in the literature. For example, a diffusion coefficient of 1.31×10^{-10} cm^2 s^{-1} was reported by Stannett *et al.*[13] for water vapour with an activity of 0.96 diffusing in PAN at 15°C. It is noted that the treatment history of the films used by Stannett *et al.* is unknown.

The results obtained here indicate the importance of film processing on subsequent diffusion behaviour. The water solubility, reflected in values of A_∞, is lowered when higher treatment temperatures are used. This may be the result of incomplete solvent removal, as the amount of residual solvent exhibits a similar dependence on the treatment temperature. The effect of residual solvent on the diffusion coefficient is less clear and suggests further study into processing effects on diffusion. It is likely that variations in the long-time diffusion coefficient are the result of a complicated concentration dependence, such as may result from clustering[13] or from interactions between the water and the residual DMF. The role clustering may play in this system is presently under investigation in our laboratory.

Another important aspect of demonstrating the validity of these results is determining the magnitude of experimental error. The confidence intervals represent the confidence in the regressed fit of the parameters. As seen in *Table 2*, the confidence interval is quite small, being limited to a maximum variation of 14% in D and 3.5% in A_∞ and an average variation of 5.75% in D and 1.05% in A_∞. These confidence intervals do not include the possibility of error in other experimentally measured values such as the thickness. The error in the film thickness measurements, which is estimated at ±33%, does not affect the value of A_∞. It does directly affect the calculation of D, and inaccuracies in the measurement of L indicate that the range of D is from $0.56D$ to $1.77D$. However, the effect of the error in L upon the evaluation of a set of experiments designed to test reproducibility is much less. It is difficult to accurately measure the film thickness in these experiments with a micrometer, but it is possible to reproduce the same (unknown) thickness with much precision by carefully repeating the same film preparation technique. The use of profilometry, optical microscopy or interferometry for obtaining the film thickness is being explored.

CONCLUSIONS

The results presented here demonstrate that the diffusion of small molecules in polymers can be successfully measured using *FT*i.r.–a.t.r. spectroscopy in combination with a suitable diffusion model. These results are not limited to the specific system of water–PAN, but are meant to demonstrate that the *FT*i.r.–a.t.r. spectroscopic approach can be used generally to measure the diffusion of liquids in polymer films. This is an important result, as the measurement of diffusion in such systems can be difficult using existing techniques. *FT*i.r.–a.t.r. spectroscopy could also be used to measure the diffusion of gases or vapours. The diffusion coefficients presented here are consistent with values for the PAN–water vapour system obtained by traditional gravimetric techniques.

The PAN–water system may not have been the most ideal system for demonstrating this technique, due to the strong concentration dependence of the diffusion coefficient. The potential difficulties presented by this, however, only serve to demonstrate the robustness of the *FT*i.r.–a.t.r. technique, as they did not impede successful measurement of diffusion.

These results also indicate several areas of further examination of the PAN–water system. These include a more extensive evaluation of the effect of film treatment on the diffusion of water. Also, an examination of water clustering may be performed through spectral deconvolution of the OH stretching region in the infra-red spectrum. This would highlight an aspect of *FT*i.r.–a.t.r. spectroscopy which was not explored here, namely the expansion of the technique to include an examination of the state of either the polymer or penetrant during diffusion, through the molecular information which is inherent in infra-red spectroscopy.

ACKNOWLEDGEMENTS

The authors gratefully acknowledge the National Science Foundation for support of the *FT*i.r. spectrometer (grant no. CTS-8908037).

REFERENCES

1 Comyn, J. in 'Polymer Permeability' (Ed. J. Comyn), Elsevier Applied Science, New York, 1985
2 Vergnaud, J. M. 'Liquid Transport Processes in Polymeric Materials: Modeling and Industrial Applications', Prentice-Hall, Englewood Cliffs, 1991
3 Vieth, W. R. and Sladek, K. *J. Colloid Sci.* 1965, **20**, 1014
4 Koros, W. J., Paul, D. R. and Rocha, A. A. *J. Polym. Sci., Polym. Phys. Edn* 1976, **14**, 687
5 Koros, W. J. and Paul, D. R. *J. Polym. Sci., Polym. Phys. Edn* 1976, **14**, 1903
6 Enscore, D. J., Hopfenberg, H. B., Berens, A. R. and Stannett, V. *Polymer* 1977, **18**, 1105
7 Hopfenberg, H. B., Stannett, V. and Jacques, C. H. M. *J. Appl. Polym. Sci.* 1975, **19**, 2439
8 Hopfenberg, H. B., Stannett, V. and Folk, G. M. *Polym. Eng. Sci.* 1975, **15**, 261
9 Harrick, N. J. *J. Opt. Soc. Am.* 1965, **55**, 851
10 Tompkins, H. G. *Appl. Spectrosc.* 1974, **28**, 335
11 Stannett, V., Haider, M., Koros, W. J. and Hopfenberg, H. B. *Polym. Eng. Sci.* 1980, **20**, 300
12 Ranade, G., Stannett, V. and Koros, W. J. *J. Appl. Polym. Sci.* 1980, **25**, 2179
13 Stannett, V. T., Ranade, G. R. and Koros, W. J. *J. Membrane Sci.* 1982, **10**, 219
14 Fester, W. in 'Polymer Handbook' (Eds J. Brandrup and E. H. Immergut), 3rd Edn, John Wiley and Sons, New York, 1989, p. V-57